J. Fluid Mech. (1969), *vol.* 37, *part* 3, *pp.* 417–434
Printed in Great Britain

On the generation of double Kelvin waves

By L. A. MYSAK

Department of Mathematics and Institute of Oceanography,
University of British Columbia, Vancouver 8, Canada

(Received 29 August 1968 and in revised form 26 December 1968)

This paper considers the linear response of a homogeneous uniformly rotating ocean of infinite horizontal extent with a discontinuity in depth to a variable horizontal wind stress. It is shown that, for either a transient or time-periodic wind stress which is suddenly applied to an initially calm sea surface, the asymptotic response far from the forcing region is dominated by an outgoing dispersive wave which is trapped along the depth discontinuity, i.e. a double Kelvin wave. Plots of the forced wave patterns in the neighbourhood of the depth discontinuity itself are also presented.

1. Introduction

The trapping of long surface waves by isolated topographical features in the ocean has been the subject of several recent investigations (Buchwald 1969; Buchwald & Adams 1968; Longuet-Higgins 1967, 1968*a*, *b*; Rhines 1967). The purpose of this paper is to report an investigation of the wind generation of one such class of waves known as double Kelvin waves or seascarp waves (see Longuet-Higgins 1968*a*). According to Longuet-Higgins, a straight discontinuity in depth in a rotating ocean can act as a wave-guide for the propagation of long waves along the discontinuity; away from the discontinuity the sea surface decays exponentially. On the basis of linearized shallow-water wave theory, it can be shown that, for any given wavelength, there is precisely one such permissible wave motion, and its period always exceeds one pendulum day, i.e. $1/f$, where f is the Coriolis parameter. Further, in a specified hemisphere, double Kelvin waves can propagate in only one direction: when $f > 0$ (< 0) the shallower (deeper) water is to the right of the direction of propagation.

In § 2 a partial differential equation for the wind-driven sea surface oscillations is derived from the equations of linearized shallow-water theory. In § 3 transform methods are used to formally solve an initial value problem for the response of the sea surface to a general space–time distribution of horizontal wind stress. The results of § 3 are then used to obtain the response to two specific wind-stress distributions: (i) a transient wind stress which has a step-function spatial dependence (§ 4) and (ii) a time-periodic wind stress which has an exponential spatial behaviour. Also, the stress fields considered in §§ 4 and 5 are non-divergent and have a component only in the direction normal to the discontinuity in depth. In each example it is shown that the asymptotic sea level response near the depth discontinuity but far from the wind-stress domain is dominated by an outgoing double Kelvin wave. In §6 plots of the wave patterns derived in §§4 and 5 are presented and discussed in some detail.

2. Basic equations

We shall assume that the motions are driven by the horizontal wind stresses alone, which in turn can be represented as body forces in the equations of motion. It is easily shown that, for normal weather systems over the deep ocean, the forcing terms in the equations of motion due to atmospheric pressure fluctuations are considerably smaller than those due to the horizontal wind stress. Further, we shall assume that the hydrostatic approximation is applicable. Then, for a homogeneous uniformly rotating fluid, the linearized non-dissipative equations expressing conservation of momentum and mass are given by

$$\left.\begin{aligned}\frac{\partial u^*}{\partial t^*}-fv^*+g\frac{\partial \xi^*}{\partial x^*}&=\frac{\tau^{x^*}}{\rho h},\\ \frac{\partial v^*}{\partial t^*}+fu^*+g\frac{\partial \xi^*}{\partial y^*}&=\frac{\tau^{y^*}}{\rho h},\end{aligned}\right\} \tag{2.1}$$

$$\frac{\partial (hu^*)}{\partial x^*}+h\frac{\partial v^*}{\partial y^*}+\frac{\partial \xi^*}{\partial t^*}=0, \tag{2.2}$$

where x^*, y^* are the Cartesian co-ordinates in the horizontal plane, t^* is the time, ξ^* is the sea surface distortion, u^*, v^* are the components of velocity in the x^*, y^* directions, h is the equilibrium depth, assumed to be a function of x^* only, f is the Coriolis parameter, g is the acceleration of gravity, ρ is the density of water, τ^{x^*}, τ^{y^*} are the components of wind stress in the x^*, y^* directions.

From (2.1) we have

$$\left.\begin{aligned}Lu^*&=-g\left(\frac{\partial^2}{\partial x^*\,\partial t^*}+f\frac{\partial}{\partial y^*}\right)\xi^*+\frac{1}{\rho h}\left(\frac{\partial \tau^{x^*}}{\partial t^*}+f\tau^{y^*}\right),\\ Lv^*&=g\left(-\frac{\partial^2}{\partial y^*\,\partial t^*}+f\frac{\partial}{\partial x^*}\right)\xi^*+\frac{1}{\rho h}\left(-f\tau^{x^*}+\frac{\partial \tau^{y^*}}{\partial t^*}\right),\end{aligned}\right\} \tag{2.3}$$

where $L=f^2+\partial^2/\partial t^{*2}$. From (2.2) and (2.3) it follows that ξ^* satisfies the equation

$$\left[h\nabla_H^{*2}\frac{\partial}{\partial t^*}+\frac{dh}{dx^*}\left(\frac{\partial^2}{\partial x^*\,\partial t^*}+f\frac{\partial}{\partial y^*}\right)-g^{-1}L\frac{\partial}{\partial t^*}\right]\xi^*=F^*, \tag{2.4}$$

where
$$F^*=\frac{1}{\rho g}\left[\nabla_H^*\cdot\frac{\partial \boldsymbol{\tau}^*}{\partial t^*}+f(\nabla^*\times\boldsymbol{\tau}^*)_{\mathbf{k}}\right].$$

We remark here that, for the particular wind-stress fields discussed in this paper, only the second term in F^* enters into the analysis (see §§4 and 5). For a barotropic study this term is more important than the horizontal divergence term, since the former is independent of the density structure in the ocean.

In (2.3) and (2.4) we now approximate L by f^2 since, for typical seascarps, double Kelvin waves have periods of several days. The physical implication of this approximation is that inertio-gravity waves do not appear in the analysis. Further, following Longuet-Higgins (1968*a*), we consider the depth profile

$$h = \begin{cases} h_1 & \text{for} \quad x^* < 0, \\ h_2 & \text{for} \quad x^* > 0, \end{cases}$$

where, without loss of generality, we assume $h_1 < h_2$. If we denote the regions $x^* < 0$ and $x^* > 0$ by the subscripts 1 and 2 respectively, (2.4) becomes

$$(\nabla_H^{*2} - f^2/gh_j)\, \xi^*_{j,t*} = F^*/h_j \quad (j = 1, 2). \tag{2.5}$$

As boundary conditions we require that ξ_1^* and ξ_2^* be bounded far from the discontinuity in depth.† At $x = 0$ we require that the surface elevation and normal transport be continuous, i.e.

$$[\xi^*]_2^1 = 0, \quad [hu^*]_2^1 = 0.$$

We now define the non-dimensional variables

$$\left.\begin{aligned} x, y = k_0(x^*, y^*), \quad & t = \sigma_0 t^*, \\ \boldsymbol{\tau} = \boldsymbol{\tau}^*/\tau_0, \quad & \xi = \xi^*/\xi_0, \end{aligned}\right\} \tag{2.6}$$

where $\xi_0 = \tau_0/\rho g h_2 k_0$ and k_0^{-1}, σ_0^{-1}, and τ_0 are respectively the length, time, and stress scales which appear in the forcing function F^*. Further, we define the non-dimensional parameters

$$\gamma = h_2/h_1 > 1, \quad \delta = \sigma_0/f > 0, \quad \epsilon = f^2/gh_2k_0^2 > 0. \tag{2.7}$$

Throughout the analysis it will be assumed, unless otherwise specified, that (i) γ is not significantly greater than unity and (ii) δ and ϵ are small compared with unity. On employing (2.6) and (2.7) in (2.5), we obtain

$$\left.\begin{aligned} (\nabla_H^2 - \epsilon\gamma)\, \xi_{1,t} &= \gamma F/\delta, \\ (\nabla_H^2 - \epsilon)\, \xi_{2,t} &= F/\delta, \end{aligned}\right\} \tag{2.8}$$

where
$$F = \delta \nabla_H \cdot \boldsymbol{\tau}_t + (\nabla \times \boldsymbol{\tau})_{\mathbf{k}}. \tag{2.9}$$

The boundary and continuity conditions now take the form

$$|\xi_1|, |\xi_2| < M \text{ (a constant)} \quad \text{as} \quad x \to -\infty, \infty \tag{2.10}$$

and
$$\left.\begin{aligned} \xi_1 = \xi_2 \quad & \text{at} \quad x = 0, \\ P(\xi_1) = \gamma P(\xi_2) \quad & \text{at} \quad x = 0, \end{aligned}\right\} \tag{2.11}$$

where
$$P = \delta\, \partial^2/\partial x\, \partial t + \partial/\partial y.$$

† In the solution for free double Kelvin waves, the appropriate boundary conditions are $\xi_1^*, \xi_2^* \to 0$ as $x^* \to -\infty, \infty$ respectively. However, the forced solution contains terms in addition to those corresponding to double Kelvin waves, so that these more general boundary conditions are imposed.

3. Sea level response to a horizontal wind stress of general form

We assume that for $t \leqslant 0$ the sea surface is at its equilibrium level, i.e.

$$\xi_j = 0 \quad \text{for} \quad t \leqslant 0 \quad (j = 1, 2), \tag{3.1}$$

and that at $t = 0$ a wind stress is suddenly applied. With these initial conditions now specified, we take Fourier and Laplace transforms of (2.8)–(2.11). Upon defining

$$\begin{Bmatrix} \bar{\xi}_j(x,k,s) \\ \bar{F}(x,k,s) \end{Bmatrix} = \int_{-\infty}^{\infty} \exp(-iky)\,dy \int_0^{\infty} \exp(-st) \begin{Bmatrix} \xi_j(x,y,t) \\ F(x,y,t) \end{Bmatrix} dt \tag{3.2}$$

and assuming that ξ_j, $\partial \xi_j/\partial y$, and $F \to 0$ as $|y| \to \infty$, equations (2.8) together with (3.1) yield

$$\left.\begin{aligned} (d^2/dx^2 - K_1^2)\,\bar{\xi}_1 &= \gamma \bar{F}/\delta s, \\ (d^2/dx^2 - K_2^2)\,\bar{\xi}_2 &= \bar{F}/\delta s, \end{aligned}\right\} \tag{3.3}$$

where $\qquad K_1 = (k^2 + \epsilon\gamma)^{\frac{1}{2}} \quad \text{and} \quad K_2 = (k^2 + \epsilon)^{\frac{1}{2}}.$

Since K_1 and K_2 are not single valued in the complex variable k, we choose the Riemann sheet for which $K_1, K_2 > 0$ when k is real. In the (x, k, s)-space the conditions (2.10) and (2.11) become

$$|\bar{\xi}_1|, |\bar{\xi}_2| < M \quad \text{as} \quad x \to -\infty, \infty \tag{3.4}$$

and

$$\left.\begin{aligned} \bar{\xi}_1 &= \bar{\xi}_2 \quad \text{at} \quad x = 0, \\ \bar{P}(\bar{\xi}_1) &= \gamma \bar{P}(\bar{\xi}_2) \quad \text{at} \quad x = 0, \end{aligned}\right\} \tag{3.5}$$

where $\bar{P} = \delta s\, d/dx + ik$. The solutions to (3.3) which satisfy (3.4) can be written in the form

$$\left.\begin{aligned} \bar{\xi}_1(x,k,s) &= A_1(k,s)\exp(K_1 x) + \bar{\xi}_{1p}(x,k,s), \\ \bar{\xi}_2(x,k,s) &= A_2(k,s)\exp(-K_2 x) + \bar{\xi}_{2p}(x,k,s), \end{aligned}\right\} \tag{3.6}$$

where $\bar{\xi}_{1p}$, $\bar{\xi}_{2p}$ are particular integrals of (3.3) which are bounded in the limit $x \to -\infty, \infty$ respectively. The unknown coefficients in (3.6), A_1 and A_2, are determined from the continuity conditions (3.5); we find that

$$\left.\begin{aligned} A_1 &= [\beta + \gamma\alpha(\delta s K_2 - ik)]/\Delta, \\ A_2 &= [\beta - \alpha(\delta s K_1 + ik)]/\Delta, \end{aligned}\right\} \tag{3.7}$$

where the functions α, β, and Δ are given by

$$\left.\begin{aligned} \alpha(k,s) &= \bar{\xi}_{2p}(0,k,s) - \bar{\xi}_{1p}(0,k,s), \\ \beta(k,s) &= ik[\gamma \bar{\xi}_{2p}(0,k,s) - \bar{\xi}_{1p}(0,k,s)] \\ &\qquad + \delta s[\gamma\, d\bar{\xi}_{2p}(0,k,s)/dx - d\bar{\xi}_{1p}(0,k,s)/dx], \\ \Delta(k,s) &= \delta s(K_1 + \gamma K_2) - ik(\gamma - 1). \end{aligned}\right\} \tag{3.8}$$

Hence the sea level response is obtained from (3.6), which are now known functions, by inverting the Fourier and Laplace transforms, viz.

$$\xi_j(x,y,t) = \frac{1}{4\pi^2 i}\int_{-\infty}^{\infty} \exp(iky)\,dk \int_{-i\infty}^{i\infty} \exp(st)\,\bar{\xi}_j(x,k,s)\,ds. \tag{3.9}$$

In (3.9) it is to be understood that the inversion path in the s plane must be indented to the right of any singularities of $\bar{\xi}_j$ which lie on the imaginary s axis. Also, the inversion path in the k-plane must be suitably indented above or below any singularities of $\bar{\xi}_j$ which lie on the real k axis; the appropriate indentations in this path are to be determined by the familiar Sommerfeld radiation condition.

4. Response to a transient wind stress

As our first example, we consider a transient wind stress which, in dimensional variables, has the form

$$\left.\begin{aligned} \tau^{x^*} &= \tau_0 H(t^*) H(y^*) \exp(-\sigma_0 t^*), \\ \tau^{y^*} &= 0, \end{aligned}\right\} \tag{4.1}$$

where σ_0, $\tau_0 > 0$ and $H(u)$ is the unit step function. This stress field could be regarded as a rough approximation to part of the wind field associated with the sudden intensification and gradual decay of a large anticyclonic weather system centred over the escarpment. In this case it is clear that we use σ_0^{-1} and τ_0 to non-dimensionalize the time and stress. However, since there is no specific length scale in (4.1), we non-dimensionalize x^* and y^* by $k_0^{-1} = (gh_2)^{\frac{1}{2}} f^{-1}$, which implies that $\epsilon = 1$ in this model (see (2.7)). From (2.9) we find that the forcing function for this problem reduces to

$$F(y,t) = -H(t)\,\delta(y)\exp(-t), \tag{4.2}$$

where $\delta(y)$ is the Dirac delta function. The application of (3.2) to (4.2) yields $\bar{F} = 1/(s+1)$. Hence the particular integrals of (3.3) are given by

$$\left.\begin{aligned} \bar{\xi}_{1p} &= \gamma/\delta s(s+1) K_1^2, \\ \bar{\xi}_{2p} &= 1/\delta s(s+1) K_2^2, \end{aligned}\right\} \tag{4.3}$$

where, in view of the choice of length scale for this problem,

$$K_1 = (k^2+\gamma)^{\frac{1}{2}}, \quad K_2 = (k^2+1)^{\frac{1}{2}}. \tag{4.4}$$

Throughout the remainder of this section, it is to be understood that the functions K_1 and K_2 take on the values defined by (4.4). From (3.7), (3.8), and (4.3) we find that

$$\left.\begin{aligned} A_1 &= \gamma B(i - \delta s k/K_2)/K_1^2, \\ A_2 &= B(i + \delta s k/K_1)/K_2^2, \end{aligned}\right\} \tag{4.5}$$

where
$$B(k,s) = (\gamma - 1)\,k/\delta s(s+1)\,\Delta.$$

Hence, from (3.9) we have

$$\left.\begin{aligned} \xi_1(x,y,t) &= (1/4\pi^2 i)\int_{-\infty}^{\infty} \exp(iky)\,dk \int_C \exp(st)\,[A_1 \exp(K_1 x) + \gamma/\delta s(s+1) K_1^2]\,ds, \\ \xi_2(x,y,t) &= (1/4\pi^2 i)\int_{-\infty}^{\infty} \exp(iky)\,dk \int_C \exp(st)\,[A_2 \exp(-K_2 x) + 1/\delta s(s+1) K_2^2]\,ds, \end{aligned}\right\} \tag{4.6}$$

where A_1 and A_2 are given by (4.5) and C denotes the path from $s = -i\infty$ to $s = i\infty$ indented to the right of $s = i\omega$, where

$$\omega(k) = (\gamma-1)k/\delta(K_1+\gamma K_2). \tag{4.7}$$

In the s plane, the only singularities of the integrands in (4.6) are the simple poles at $s = 0, -1$, and $i\omega$; hence the Laplace inversion is straightforward and we do this first. For $t > 0$ we thus obtain

$$\begin{aligned}\xi_1 = {} & (\gamma/2\pi\delta)\int_{-\infty}^{\infty} dk \exp(iky)\,[1-\exp(K_1 x)]/K_1^2 \\ & +[\gamma\exp(-t)/2\pi\delta]\int_{-\infty}^{\infty} dk \exp(iky) \\ & \qquad \times [k(\gamma-1)(iK_2+\delta k)\exp(K_1 x)/DK_2-1]/K_1^2 \\ & +(\gamma/2\pi)\int_{-\infty}^{\infty} dk \exp[i(ky+\omega t)+K_1 x]\,(K_1+K_2)/DK_1K_2, \end{aligned} \tag{4.8}$$

$$\begin{aligned}\xi_2 = {} & (1/2\pi\delta)\int_{-\infty}^{\infty} dk \exp(iky)\,[1-\exp(-K_2 x)]/K_2^2 \\ & +(\exp(-t)/2\pi\delta)\int_{-\infty}^{\infty} dk \exp(iky) \\ & \qquad \times [k(\gamma-1)(iK_1-\delta k)\exp(-K_2 x)/DK_1-1]/K_2^2 \\ & +(\gamma/2\pi)\int_{-\infty}^{\infty} dk \exp[i(ky+\omega t)-K_2 x]\,(K_1+K_2)/DK_1K_2. \end{aligned} \tag{4.9}$$

For $t \leqslant 0$, we have $\xi_j = 0$ $(j = 1, 2)$. In (4.8) and (4.9) the function D is defined by

$$D(k) = \delta(K_1+\gamma K_2)+ik(\gamma-1).$$

From (4.8) and (4.9) we note that in each region the response consists of the superposition of steady-state, transient, and wave-like terms. Most of the integrals which appear in (4.8) and (4.9) cannot be evaluated in terms of known functions. Thus, for a complete description of the forced sea level behaviour, several numerical integrations would be required. We shall not present any such computations at this stage, however; we shall discuss instead the asymptotic behaviour of the solution, which in itself is fairly instructive. For $y \gg 1$ and x of order unity each contribution to ξ_1 and ξ_2 is exponentially small. This is also true for $-y \gg 1$ with the exception of the wave-like integrals which contribute terms of order $(-y)^{-\frac{1}{2}}$ when both $-y \gg 1$ and $t \gg 1$. In each region these dominating terms, when combined appropriately, represent a double Kelvin wave progressing in the negative y direction; away from the discontinuity the wave amplitude decays exponentially. It is important to note that if $\gamma = 1$, which corresponds to an ocean of uniform depth, there is no such trapped wave in the solution (see (4.7)).

We now discuss in some detail the asymptotic sea level behaviour in the neighbourhood of the discontinuity itself, where the amplitude of the response is a maximum. From (4.8) and (4.9) we have

$$\begin{aligned}\xi(0,y,t) &= \xi_1(0-,y,t) = \xi_2(0+,y,t) \\ &= \xi_T+\xi_W, \end{aligned} \tag{4.10}$$

where
$$\xi_T(y,t) = -\exp(-t)\int_{-\infty}^{\infty} \exp(iky)\,g(k)\,dk, \tag{4.11}$$
$$\xi_W(y,t) = \int_{-\infty}^{\infty} \exp[i(ky+\omega(k)t)]\,g(k)\,dk, \tag{4.12}$$
in which
$$g(k) = \gamma(K_1+K_2)/2\pi D K_1 K_2.$$
In the k plane, $g(k)$ and $\omega(k)$ have branch points at $k = \pm i$ and $k = \pm i\gamma^{\frac{1}{2}}$. Since the inversion path is along the real axis, we extend the branch cuts out to infinity

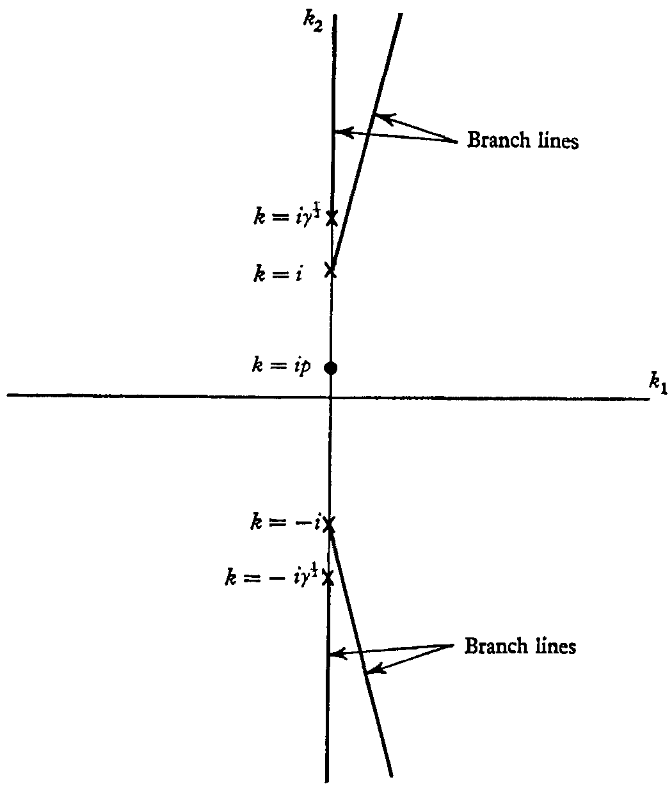

FIGURE 1. Diagram showing the location of the branch points, branch lines, and pole in the k plane, where $k = k_1 + ik_2$.

in the first and fourth quadrants (see figure 1). Further, $g(k)$ has a simple pole at $k = ip$, where $D(k)$ vanishes; for $0 < \delta \ll 1$, $p \simeq \gamma^{\frac{1}{2}}\delta/(\gamma^{\frac{1}{2}}-1) > 0$. The asymptotic behaviour of ξ_T for $|y| \gg 1$ can be found fairly easily by Laplace's method (for an excellent discussion of this method, see Carrier, Krook & Pearson 1966, chapter 6). It follows from (4.11) that, for $0 < \delta \ll 1$,
$$\begin{aligned}\xi_T \sim & -H(y)\,\gamma^{\frac{1}{2}}(\gamma^{\frac{1}{2}}-1)^{-1}\exp(-py-t) \\ & + \operatorname{sgn}(y)\,\gamma(\gamma-1)^{-1}(2\pi|y|)^{-\frac{1}{2}} \\ & \qquad \times [\exp(-t-|y|) + \gamma^{-\frac{3}{4}}\exp(-t-\gamma^{\frac{1}{2}}|y|)] \\ & + O[|y|^{-\frac{3}{2}}\exp(-|y|)] \quad (|y| \gg 1). \end{aligned} \tag{4.13}$$

The first term in (4.13) represents the contribution due to the pole at $k = ip$; the remaining terms arise from integrating around the branch cuts. Before discussing the asymptotic behaviour of ξ_W, we first rewrite (4.12) in the form

$$\xi_W = \int_{-\infty}^{\infty} \exp\left[-yf(k)\right] g(k)\, dk, \tag{4.14}$$

where
$$f(k) = -i[k+\beta\omega(k)], \tag{4.15}$$

in which $\beta = t/y$. We now use the method of steepest descent to determine the behaviour of (4.14) for large $|y|$ and t. In the appendix it is shown that, for $0 < \delta \ll 1$ and $(\gamma-1)\beta = O(1)$, $f(k)$ as defined by (4.15) has saddle-points only if $\beta < 0$, i.e. only if $y < 0$. Further, there are precisely two saddle-points when $y < 0$, and these satisfy the equation

$$d\omega/dk = -1/\beta > 0. \tag{4.16}$$

It follows that the dominant contributions to (4.14) arise from the neighbourhood of those k values which satisfy (4.16); the quantity $-1/\beta$, of course, represents the group velocity associated with each of these wave-numbers. Thus, for $y < 0$ we find (see appendix for details) that

$$\xi_W \sim \frac{4\gamma^{\frac{1}{4}}[\delta(\gamma-1)\sin Q-(\gamma+1)\cos Q]}{(-2\pi y)^{\frac{1}{2}}\, m^{\frac{3}{2}}[(\gamma-1)^{\frac{1}{2}}+\delta^2(\gamma+1)^2]} \quad (-y \gg 1 \quad \text{and} \quad t \gg 1), \tag{4.17}$$

where
$$\left.\begin{aligned} m &= [-2(\gamma-1)\beta/\delta\gamma^{\frac{1}{2}}(\gamma+1)^2]^{\frac{1}{3}}, \\ Q &= m\gamma^{\frac{1}{2}}y+(\gamma-1)t/(\gamma+1)\delta+\pi/4. \end{aligned}\right\} \tag{4.18}$$

For $y > 0$, however, ξ_W behaves like

$$\xi_W \sim \gamma^{\frac{1}{2}}(\gamma^{\frac{1}{2}}-1)^{-1}\exp(-py-t)+O[y^{-\frac{3}{2}}\exp(-y)] \quad (y \gg 1). \tag{4.19}$$

From (4.10), (4.13), (4.17) and (4.19) we consequently have that the asymptotic sea level response at the depth discontinuity is given by

$$\left.\begin{aligned} \xi(0,y,t) &\sim \frac{4\gamma^{\frac{1}{4}}\sin(Q-\phi)}{(-2\pi y)^{\frac{1}{2}}\, m^{\frac{3}{2}}[(\gamma-1)^2+\delta^2(\gamma+1)^2]^{\frac{1}{2}}} \quad (-y \gg 1 \quad \text{and} \quad t \gg 1), \\ &\sim O[y^{-\frac{3}{2}}\exp(-y)] \quad (y \gg 1), \end{aligned}\right\} \tag{4.20}$$

where
$$\phi = \cot^{-1}[\delta(\gamma+1)/(\gamma-1)].$$

We note from (4.20) that the asymptotic response is dominated by a dispersive wave which propagates away from the region where the wind stress is applied. For small changes in t and fixed $y < 0$, this wave has a period of approximately $(\gamma+1)/(\gamma-1)$ pendulum days (see (4.18)), which corresponds to the period of a free non-divergent double Kelvin wave (see Longuet-Higgins 1968*a*). For plots of the function $\xi(0,y,t)$ and a further discussion of the solution, the reader is referred to §6.

5. Response to a time-periodic wind stress

We now consider the response to a time-periodic wind stress of the form

$$\left.\begin{aligned} \tau^{x^*} &= \tfrac{1}{2}\tau_0 H(t^*)\cos(\sigma_0 t^*)\exp(-k_0|y^*|), \\ \tau^{y^*} &= 0, \end{aligned}\right\} \tag{5.1}$$

where $\sigma_0, k_0, \tau_0 > 0$. This stress field could be regarded as a rough approximation to fluctuating winds caused by alternating anticyclonic and cyclonic weather systems. In this example we non-dimensionalize the distance, time and stress by k_0^{-1}, σ_0^{-1} and τ_0 respectively. The forcing function (2.9) which corresponds to (5.1) is given by

$$F(y,t) = \tfrac{1}{2}H(t)\,\mathrm{sgn}\,(y)\exp(-|y|)\,\mathrm{Re}\,[\exp(it)]. \tag{5.2}$$

Following the procedure outlined in §3, the response to the forcing function (5.2) is again easily obtained as a linear combination of Fourier integrals. For the sake of brevity, however, we shall not present all the details of the solution since it is quite similar in form to the solution given by (4.8) and (4.9). For example, the response to (5.2) in the region $x > 0$ is given by the real part of the following expression:

$$\begin{aligned} \xi_2 = &-\int_{-\infty}^{\infty} dk\exp(iky)\,[1-\exp(-K_2 x)]\,h/K_2^2 \\ &+\exp(it)\int_{-\infty}^{\infty} dk\exp(iky)\,h/K_2^2 \\ &-\exp(it)\int_{\Gamma} dk\exp(iky-K_2 x)\,hk(\gamma-1)\,(K_1+\delta k)/EK_1K_2^2 \\ &+\gamma\delta\int_{\Gamma} dk\exp[i(ky+\omega t)-K_2 x]\,(K_1+K_2)\,h/EK_1K_2, \end{aligned}$$

where

$$\begin{aligned} h(k) &= k/2\pi\delta(k^2+1), \\ \omega(k) &= k(\gamma-1)/\delta(K_1+\gamma K_2), \\ E(k) &= k(\gamma-1)-\delta(K_1+\gamma K_2), \end{aligned}$$

and Γ denotes the path from $k = -\infty$ to $k = +\infty$ indented above the pole at $k = q > 0$; for small δ and ϵ, $q \simeq \delta(\gamma\epsilon)^{\frac{1}{2}}(\gamma^{\frac{1}{2}}-1)$. With this choice for Γ, the radiation condition is automatically satisfied.

The most significant difference between the two solutions is that large amplification of the sea level response (i.e. resonance) can now occur since $F(y,t)$ is periodic in time (see below). The asymptotic response at the depth discontinuity is given by

$$\xi(0,y,t) \sim \frac{\gamma\exp(-y)}{(\gamma-1)-\delta(\gamma+1)}\left\{\sin\left[\frac{(\gamma-1)t}{(\gamma+1)\delta}\right]-\sin(t)\right\} \quad (y \gg 1), \tag{5.3}$$

$$\begin{aligned} \xi(0,y,t) \sim &\frac{4\gamma(\gamma-1)\sin(R)}{(-2\pi nby)^{\frac{1}{2}}(1+n^2b^2)\,[(\gamma-1)^2-\delta^2(\gamma+1)^2]} \\ &-\frac{\gamma\exp(y)}{(\gamma-1)+\delta(\gamma+1)}\left\{\sin\left[\frac{(\gamma-1)t}{(\gamma+1)\delta}\right]+\sin(t)\right\} \quad (-y \gg 1 \quad \text{and} \quad t \gg 1), \end{aligned} \tag{5.4}$$

where
$$\left.\begin{aligned} b &= (\epsilon\gamma)^{\frac{1}{2}}, \\ n &= [-2(\gamma-1)\beta/\delta b(\gamma+1)^2]^{\frac{1}{3}}, \\ R &= nby+(\gamma-1)t/(\gamma+1)\delta+\tfrac{1}{4}\pi. \end{aligned}\right\} \tag{5.5}$$

From (5.3) and (5.4) we note that, provided $\delta = \sigma_0/f \neq (\gamma-1)/(\gamma+1)$, the response is exponentially small except for the double Kelvin wave travelling in the negative y direction. As in the previous example, its period is approximately given by $(\gamma+1)/(\gamma-1)$ pendulum days; its amplitude, however, falls off like $(-y)^{-\frac{1}{3}}$ (see (5.4) and (5.5)). Finally, in the limit $\sigma_0 \to \sigma^* \equiv f(\gamma-1)/(\gamma+1)$, it is easily seen that resonance occurs: for $y > 0$ the response behaves like $t\cos(t)$ as $\sigma_0 \to \sigma^*$; for $y < 0$ on the other hand, only the double Kelvin wave is amplified and its amplitude behaves like $(\sigma_0-\sigma^*)^{-1}$ as $\sigma_0 \to \sigma^*$.

6. Graphs of the response at $x = 0$

To gain a deeper understanding of the wave motions associated with the solutions obtained in §§4 and 5, we shall now present a number of figures which depict the sea level response $\xi(0, y, t)$ at successive instants of time. In the calculations for the wave profiles illustrated below we have set

$$\gamma = h_2/h_1 = \tfrac{4}{3} \quad \text{and} \quad f = 0{\cdot}9 \times 10^{-4}\,\text{sec}^{-1}.$$

These values for the depth ratio and Coriolis parameter are appropriate for the Mendocino escarpment off the Californian coast where double Kelvin waves might exist. This seascarp, which is centred at about 40° N latitude, extends westward for nearly 3000 km, with the shallower water to the north. According to the theory, double Kelvin waves should progress westwards, or, in terms of the co-ordinate system used in the present analysis, in the negative y direction. However, since the seascarp model discussed in this paper is of infinite horizontal extent and other important effects such as density stratification and bottom friction have been neglected, we must be cautious in applying the above theory directly to a region in the ocean such as the Mendocino escarpment. In view of these and other shortcomings (see §7) in the theory, perhaps the most that should be inferred from the numerical results presented below are rough estimates of the wave amplitude and period, wavelength and current velocities associated with double Kelvin waves in the real ocean.

Figure 2 shows the asymptotic wave height (4.20) as a function of position at successive instants of time. In (4.20) we have set $\delta = 0{\cdot}05$ ($\sigma_0 = 0{\cdot}45 \times 10^{-5}\,\text{sec}^{-1}$); hence $t_2 - t_1 = 0{\cdot}5$ corresponds to a dimensional time lapse of about 1·2 days. From figure 2 the following properties of the wave motion should be noted: (i) for fixed t, the wavelength slowly increases with increasing negative y; (ii) as t increases, the wavelength slowly decreases; and (iii) as t increases, the amplitude slowly decreases. We also note from figure 2 that the asymptotic wave period is about six days, which, for the given values of γ and f, is roughly the same as the period, T, of a free non-divergent double Kelvin wave, which is given by $T = 2\pi(\gamma+1)/(\gamma-1)f$. To determine the nature of the response for small t and to check the asymptotic solution defined by (4.20), the function $\xi(0, y, t)$ defined

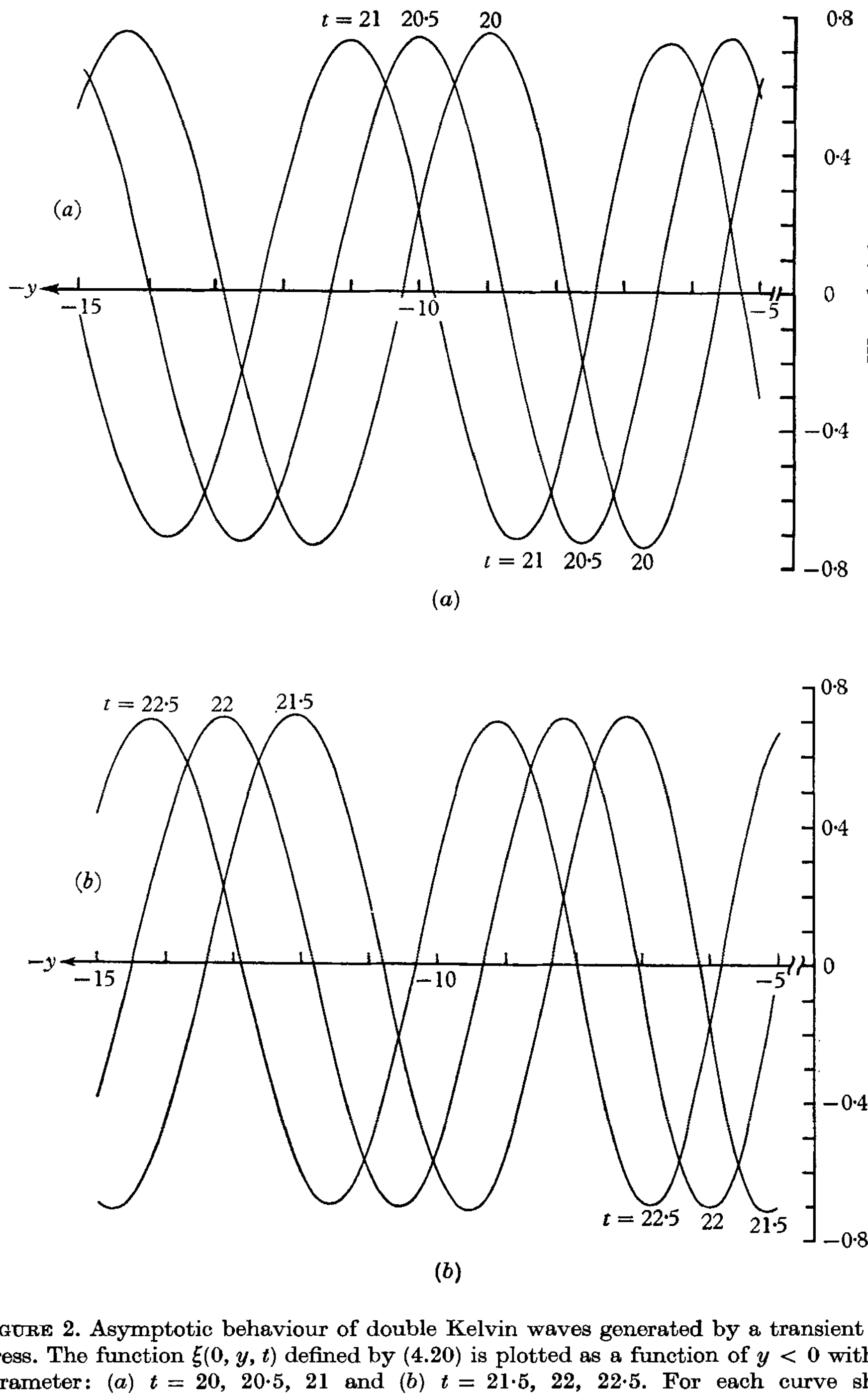

FIGURE 2. Asymptotic behaviour of double Kelvin waves generated by a transient wind stress. The function $\xi(0, y, t)$ defined by (4.20) is plotted as a function of $y < 0$ with t as parameter: (*a*) $t = 20$, $20{\cdot}5$, 21 and (*b*) $t = 21{\cdot}5$, 22, $22{\cdot}5$. For each curve shown, $\gamma = 1{\cdot}33$ and $\delta = 0{\cdot}05$.

by (4.10)–(4.12) was computed by standard numerical integration methods. Since $g(k)$ (see (4.11) and (4.12)) falls off like $1/k^2$ as $k \to \infty$, the range of integration used in the computations was $|k| \leqslant 30$; it was found that this truncation introduced an error of less than 0·1 %. From figures 3 (*a*) and 3 (*b*) we note that, shortly

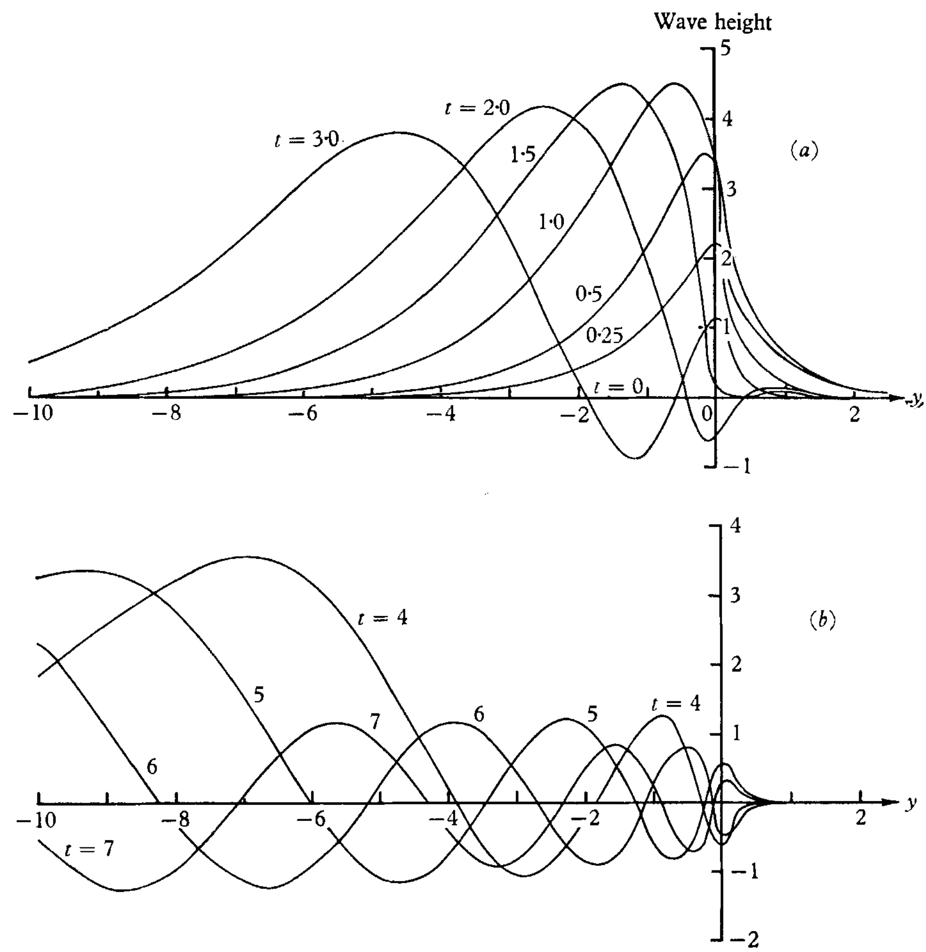

FIGURE 3. Sea level response (wave height) due to a transient wind stress. The function $\xi(0, y, t)$ defined by (4.10) is plotted as a function of y with t as parameter: (*a*) $t = 0$, 0·25, 0·5, 1, 2, 3; (*b*) $t = 4$, 5, 6, 7; (*c*) $t = 8$, 10, 15; (*d*) $t = 20$, 21; (*e*) $t = 25$, 50. For each curve shown, $\gamma = 1{\cdot}33$ and $\delta = 0{\cdot}05$. Dashed lines in (*c*), (*d*), and (*e*): the asymptotic response defined by (4.20) for $t = 15$, 20, 21 and 25.

after the wind stress is applied, a single wave of fairly large amplitude is generated in the neighbourhood of $y = 0$; as t increases, this wave progresses in the negative y direction, away from the wind stress domain ($y > 0$). For $t > 3$, after which time the wind stress and transient parts of the solution defined by (4.11) are both very small, several more progressive waves are successively generated near the origin; these 'secondary waves', however, are characterized by a much smaller amplitude and shorter wavelength than those associated with the 'initial wave'.

It is instructive to note that the three properties of the response which were inferred from the asymptotic solution are confirmed by the numerical solution for large t (see figures 3(*c*)–(*e*)). The agreement between the asymptotic and numerical solutions for $-10 \leqslant y \leqslant -5$ and $t \gg 1$ is fairly good only for $t = 20$ and 21, however, for which cases $-(\gamma-1)\beta \simeq 1$. This is not surprising in view of the fact that this condition was used in the derivation of (4.20).

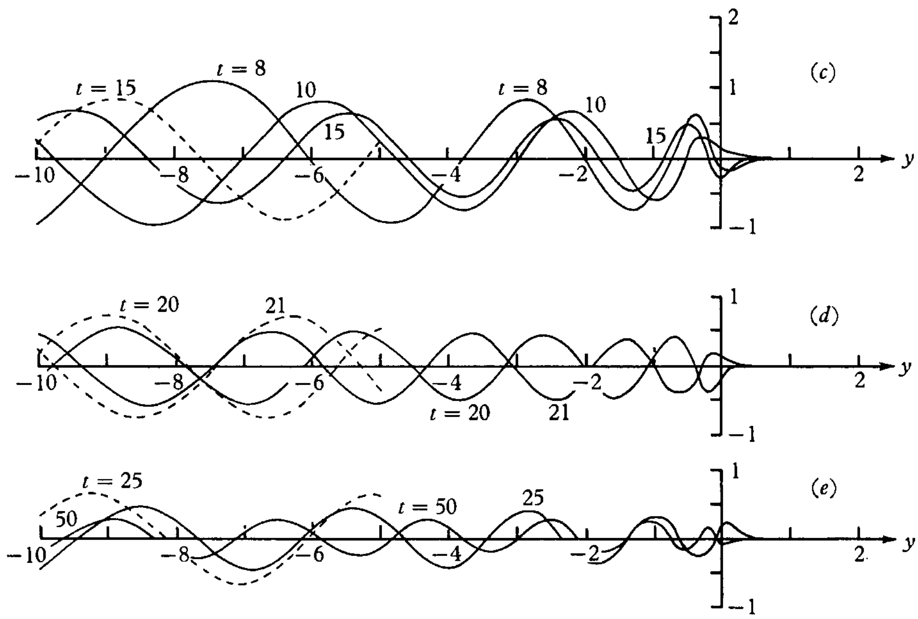

Fig. 3 (*c*–*e*). For legend see facing page.

Figure 4 shows the asymptotic wave height defined by (5.4) at successive instants of time. In this case we have set $\delta = 0{\cdot}1$ and $\epsilon = 0{\cdot}1$, which implies that $\sigma_0 = 0{\cdot}9 \times 10^{-5}\,\mathrm{sec}^{-1}$ (i.e. a forcing period of about 8 days) and $k_0 = 1{\cdot}3 \times 10^{-8}\,\mathrm{cm}^{-1}$. In contrast to the asymptotic response due to a transient wind stress, we note that for fixed $t \gg 1$ the wave height slowly decays with negative y. The wavelength dependence on y and t, however, is similar to that shown in figure 2. Finally, we note that the asymptotic wave period is again about 6 days.

We conclude this section by giving estimates of the amplitude, wavelength and current velocities associated with the waves generated by each of the wind-stress models. For the transient wind-stress case, we find that, for $\tau_0 = 3\,\mathrm{dynes\,cm}^{-2}$, $k_0 = f(gh_2)^{-\frac{1}{2}} = 0{\cdot}4 \times 10^{-8}\,\mathrm{cm}^{-1}$ (corresponding to $f = 0{\cdot}9 \times 10^{-4}\,\mathrm{sec}^{-1}$, $g = 10^3\,\mathrm{cm\,sec}^{-2}$, and $h_2 = 5 \times 10^5\,\mathrm{cm}$), $\xi_0 = \tau_0(\rho g h_2 k_0)^{-1} \simeq 1{\cdot}5\,\mathrm{cm}$. Hence the initial wave has an amplitude of about 10 cm and a wavelength of about 10^9 cm; also, from (2.3) it follows that the associated current velocities are about $1\,\mathrm{cm\,sec}^{-1}$. The secondary waves, on the other hand, are characterized by an amplitude of about 2 cm, a wavelength of about 5×10^8 cm, and current velocities of about $0{\cdot}2\,\mathrm{cm\,sec}^{-1}$. For the time-periodic wind stress case, we find that $\xi_0 \simeq 0{\cdot}5$ cm. Hence in this case the waves are characterized by an amplitude of about 2 cm, a wavelength of about 10^9 cm, and current velocities of about 1 cm sec^{-1}. In particular we note that the characteristic wavelengths given above are somewhat longer than the total horizontal extent of the Mendocino escarpment (3×10^8 cm). It is thus evident that a seascarp model of infinite horizontal extent is not very realistic as far as the real ocean is concerned. Possible modifications of the theory in this connexion are discussed in §7.

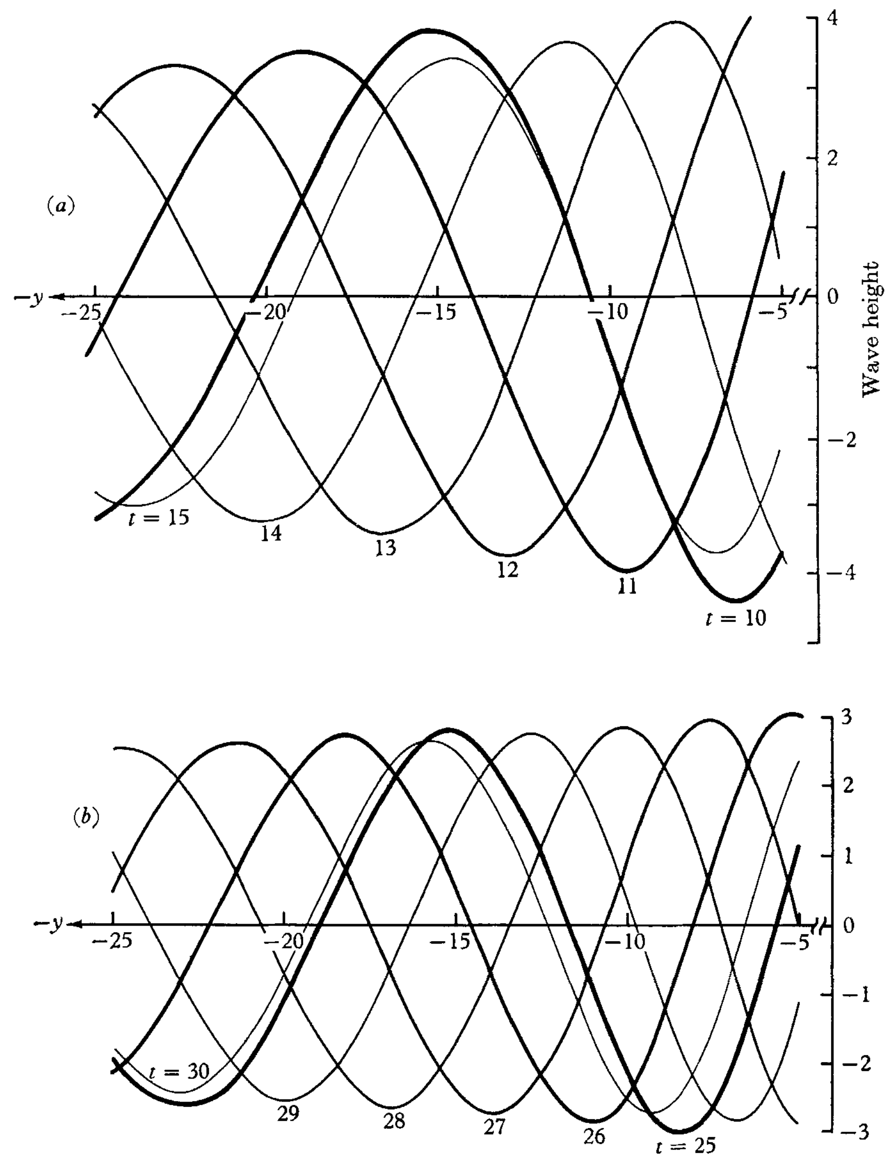

FIGURE 4. Asymptotic behaviour of double Kelvin waves generated by a time-periodic wind stress. The function $\xi(0, y, t)$ defined by (5.4) is plotted as a function of $y < 0$ with t as parameter: (a) $t = 10, 11, \ldots, 15$ and (b) $t = 25, 26, \ldots, 30$. For each curve shown, $\gamma = 1{\cdot}33$, $\delta = 0{\cdot}1$, and $\epsilon = 0{\cdot}1$.

7. Concluding remarks

We have shown that a transient or time-periodic wind stress which is suddenly applied to an unbounded ocean with a discontinuous depth profile of infinite horizontal extent can generate double Kelvin waves which travel away from the forcing region. The stress fields considered in this paper, however, are rather specialized; in each example the stress vector is nondivergent and has a component only in the direction normal to the discontinuity in depth. Also, we have not discussed here the interesting case of the response to a stress field which represents a travelling disturbance.

Further, the discontinuous depth profile considered in this paper is a rather crude approximation to a seascarp in the real ocean. Longuet-Higgins (1968*b*) has recently investigated the properties of free waves which are trapped along a seascarp with a continuous and monotonic depth profile which is asymptotic to the uniform depths h_1 and h_2. For this smooth depth profile he has shown that (i) an infinite set of trapped progressive waves can exist and (ii), as the width of the transition region tends to zero, the lowest-mode wave reduces to a double Kelvin wave while the higher-mode waves degenerate into steady currents. It would be interesting to determine whether this complete spectrum of waves could be excited by wind stress fields of the form considered in this paper, and, if so, whether the response near the escarpment is dominated by the lowest-mode wave.

As noted in the previous section, a seascarp of infinite horizontal extent may also be a rather poor approximation to a seascarp in the real ocean. An alternative and also very interesting model that could be considered for the depth profile is the following:

$$h(x) = \begin{cases} h_1 & \text{for} \quad x < 0 \quad \text{and} \quad y > 0 \\ h_2\ (> h_1) & \text{for all other } x \text{ and } y, \end{cases}$$

where y is measured positive in the eastward direction. For this geometry and a constant f plane, a double Kelvin wave travelling in the negative y direction could not exist in the region $y < 0$ but would propagate around the corner at $x = y = 0$. On the other hand, if a β plane was used along with the above geometry, some of the energy associated with a westward-travelling double Kelvin wave would be transferred (at $x = 0$) to a westward-travelling Rossby wave, which, it is well known, could exist in the region $y < 0$ (a region of uniform depth).

Finally, it would be interesting to determine the effects of stratification on the purely barotropic motions discussed here. It is not inconceivable that a significant amount of long-period energy would also be propagated by internal waves. The answer to this question is particularly important if a study to detect double Kelvin waves from deep-sea buoy measurements is undertaken.

This work was carried out during a recent visit (summer 1968) at Oregon State University, Corvallis. I am indebted to Prof. M. S. Longuet-Higgins for suggesting this investigation and for stimulating discussions. I should also like to thank Mr D. E. Kissell for his assistance with the numerical computations and the preparation of the figures. Finally, the support of the National Science Foundation through NSF Grant GA-1452 is gratefully acknowledged.

Appendix

Before applying the method of steepest descent to (4.14), it is first convenient to make the substitution

$$k = -i\gamma^{\frac{1}{2}}\sin\theta, \tag{A 1}$$

where $k = k_1 + ik_2$ and $\theta = \theta_1 + i\theta_2$. The transformation (A 1) maps the cut k plane, illustrated in figure 1, onto the strip $|\theta_1| < \frac{1}{2}\pi$, illustrated in figure 5. From (A 1), (4.14) and (4.15) we obtain

$$\xi_W = \int_{-i\infty}^{i\infty} \exp[-yF(\theta)]\, G(\theta)\, d\theta, \tag{A 2}$$

where
$$F(\theta) = -\gamma^{\frac{1}{2}}\sin\theta - \frac{(\gamma-1)\beta\sin\theta}{\delta(\cos\theta + a(\theta))},$$

$$G(\theta) = \frac{-i\gamma^{\frac{1}{2}}(\gamma\cos\theta + a(\theta))}{2\pi a(\theta)\,[\delta(\cos\theta + a(\theta)) + (\gamma-1)\sin\theta]},$$

in which
$$a(\theta) = (\gamma - \gamma^2\sin^2\theta)^{\frac{1}{2}}. \tag{A 3}$$

$F(\theta)$ and $G(\theta)$ have branch points at $\theta = \pm\theta_0 \equiv \pm\sin^{-1}(\gamma^{-\frac{1}{2}})$, which are the images of the branch points at $k = \pm i$; $G(\theta)$ has a simple pole at $-\theta \simeq \delta(\gamma^{\frac{1}{2}} - 1)^{-1} \equiv \theta_p$, which is the image of the pole at $k = ip$. The appropriate branch lines in the θ plane are shown in figure 5.

The saddle-points of $F(\theta)$ are given by $F'(\theta) = 0$, or, equivalently, by the roots of the equation

$$\delta\gamma^{\frac{1}{2}}\cos\theta[a(\cos^2\theta + a^2) + 2a^2\cos\theta] + (\gamma-1)\beta(\gamma\cos\theta + a) = 0. \tag{A 4}$$

For $0 < \delta \ll 1$ and $(\gamma-1)\beta = O(1)$, it is obvious that (A 4) has no real roots. However, if $\theta = i\theta_2$ and $\cosh\theta_2$ and $\sinh\theta_2$ are significantly greater than unity, then, provided $\beta < 0$, (A 4) has a root at $\theta = is_0$, say, where $s_0 > 0$. Upon approximating $a(is_0)$ by $\gamma\sinh s_0$ (see (A 3))† and also $\cosh s_0$ and $\sinh s_0$ by $\exp(s_0)/2$, it is easily shown that

$$s_0 \simeq \tfrac{1}{3}\log\left[\frac{-16\beta(\gamma-1)}{\delta\gamma^{\frac{1}{2}}(\gamma+1)^2}\right].$$

Since (A 4) is an even function of θ, it follows that $F(\theta)$ also has a saddle-point at $\theta = -is_0$.

The path of steepest descent through $\theta = is_0$, which we denote by C_+, satisfies the equation

$$\begin{aligned} \mathrm{Im}[F(\theta)] &= \mathrm{Im}[F(is_0)] \\ &\simeq -\gamma^{\frac{1}{2}}m - \beta(\gamma-1)/(\gamma+1)\delta, \end{aligned} \tag{A 5}$$

where
$$m = [-2\beta(\gamma-1)/\delta\gamma^{\frac{1}{2}}(\gamma+1)^2]^{\frac{1}{3}},$$

$$\mathrm{Im}[F(\theta)] = -\gamma^{\frac{1}{2}}\cos\theta_1\sinh\theta_2$$
$$-\frac{\beta(\gamma-1)}{\delta}\left[\frac{\sinh\theta_2\cosh\theta_2 + \rho(\cos\alpha\cos\theta_1\sinh\theta_2 - \sin\alpha\sin\theta_1\cosh\theta_2)}{\rho^2 + 2\rho(\cos\alpha\cos\theta_1\cosh\theta_2 - \sin\alpha\sin\theta_1\sinh\theta_2) + \cos^2\theta_1 + \sinh^2\theta_2}\right],$$

† The consequence of this approximation is that the asymptotic wave motion is, in a certain sense, non-divergent (see discussion following (4.20)).

in which α and ρ are given by

$$\tan 2\alpha = \frac{-\gamma^2 \sin 2\theta_1 \sinh 2\theta_2}{2\gamma + \gamma^2(\cos 2\theta_1 \cosh 2\theta_2 - 1)} \quad (|\alpha| < \tfrac{1}{4}\pi),$$

$$\rho = 2^{-\frac{1}{2}}\{[2\gamma + \gamma^2(\cos 2\theta_1 \cosh 2\theta_2 - 1)]^2 + \gamma^4 \sin^2 2\theta_1 \sinh^2 2\theta_2\}^{\frac{1}{4}}.$$

Since $F''(is_0) \simeq i\gamma^{\frac{1}{2}}m$, it follows that C_+ makes an angle of $\frac{1}{4}\pi$ with the imaginary axis. Also, it can be shown from (A 5) that C_+ does not cross the real axis but again crosses the imaginary axis at $\theta = i\theta_c$, where $\theta_c > 0$ and $\theta_c^2 \ll 1$; at $\theta = i\theta_c$, C_+ makes an angle of $\frac{1}{2}\pi$ with the imaginary axis. Finally, it can be shown that, as

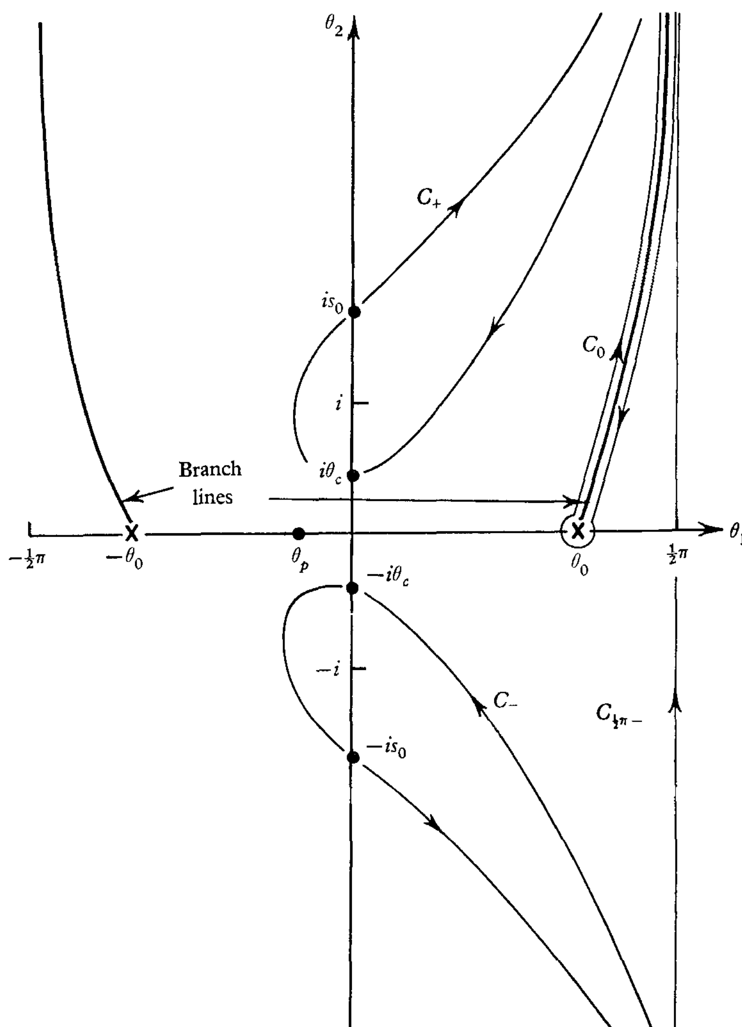

FIGURE 5. Diagram of the θ plane, where $\theta = \theta_1 + i\theta_2$. The curves C_+ and C_- are the paths of steepest descent through the saddle-points $\theta = is_0$ and $\theta = -is_0$ respectively.

$\theta_2 \to \infty$, C_+ has the line $\theta_1 = \frac{1}{2}\pi$ as the asymptote. The path through $\theta = -is_0$, which we denote by C_-, satisfies the equation

$$\mathrm{Im}\,[F(\theta)] \simeq \gamma^{\frac{1}{2}} m + \beta(\gamma-1)/(\gamma+1)\,\delta.$$

It is fairly easy to show that C_- is merely the reflexion of C_+ across the real axis. The paths C_+ and C_- are illustrated in figure 5.

Now, by Cauchy's theorem and Jordan's lemma, it follows from (A 2) that

$$\xi_W = \left\{\int_{C_+} - \int_{C_-} + \int_{C_0} + \int_{C_{\frac{1}{2}\pi-}}\right\} \exp\left[-yF(\theta)\right] G(\theta)\, d\theta,$$

where C_0 and $C_{\frac{1}{2}\pi-}$ are the paths shown in figure 5. The contributions from the integrals along C_0 and $C_{\frac{1}{2}\pi-}$ are of order $(-y)^{-\frac{1}{2}} \exp(y)$ and for $-y \gg 1$ are very small in comparison with the contributions along C_+ and C_- in the neighbourhood of the saddle-points. We thus find that, for $-y \gg 1$ and $t \gg 1$, the leading terms of the asymptotic representation of ξ_W are given by

$$\xi_W \sim \left(\frac{2\pi}{-y}\right)^{\frac{1}{2}} \left\{\frac{G(is_0)\exp\left[-yF(is_0) + \frac{1}{4}i\pi\right]}{|F''(is_0)|} - \frac{G(-is_0)\exp\left[-yF(-is_0) - \frac{1}{4}i\pi\right]}{|F''(-is_0)|}\right\}. \tag{A 6}$$

Upon making the appropriate substitutions, (A 6) reduces to (4.17).

REFERENCES

Buchwald, V. T. 1969 Long waves on oceanic ridges. *Proc. Roy. Soc.* A **308**, 343–54.

Buchwald, V. T. & Adams, J. K. 1968 The propagation of continental shelf waves. *Proc. Roy. Soc.* A **305**, 235–50.

Carrier, G. F., Krook, M. & Pearson, C. E. 1966 *Functions of a Complex Variable*. New York: McGraw-Hill.

Longuet-Higgins, M. S. 1967 On the trappings of wave energy round islands. *J. Fluid Mech.* **29**, 781–821.

Longuet-Higgins, M. S. 1968*a* On the trapping of waves along a discontinuity of depth in a rotating ocean. *J. Fluid Mech.* **31**, 417–34.

Longuet-Higgins, M. S. 1968*b* Double Kelvin waves with continuous depth profiles. *J. Fluid Mech.* **34**, 49–80.

Rhines, P. B. 1967 Slow oscillations in an ocean of varying depth. Ph.D. dissertation, Cambridge University.